0026-895X/07/7101-193–200$20.00
MOLECULAR PHARMACOLOGY
Copyright © 2007 The American Society for Pharmacology and Experimental Therapeutics
*Mol Pharmacol* 71:193–200, 2007

Vol. 71, No. 1
28407/3160773
*Printed in U.S.A.*



# Motexafin Gadolinium-Induced Cell Death Correlates with Heme oxygenase-1 Expression and Inhibition of P450 Reductase-Dependent Activities

John P. Evans, Fengyun Xu, Mint Sirisawad, Richard Miller, Louie Naumovski, and Paul R. Ortiz de Montellano

*Department of Pharmaceutical Chemistry, University of California, San Francisco, California (J.P.E., F.X., P.R.O.M.); and Pharmacyclics, Inc., Sunnyvale, California (M.S., R.M., L.N.)*

Received June 28, 2006; accepted October 3, 2006

## ABSTRACT

Heme oxygenase-1 (HO1), which oxidizes heme to biliverdin, CO, and free iron, conveys protection against oxidative stress and is antiapoptotic. Under stress conditions, some porphyrin derivatives can inhibit HO1 and trigger cell death. Motexafin gadolinium (MGd) is an expanded porphyrin that selectively targets cancer cells through a process of futile redox cycling that decreases intracellular reducing metabolites and protein thiols. Here, we report that hematopoietic-derived cell lines that constitutively express HO1 are more susceptible to MGd-induced apoptosis than those that do not. MGd used in combination with tin protoporphyrin IX, an inhibitor of HO1, resulted in synergistic cell killing. Consistent with these cell culture observations, we found that MGd is an inhibitor of heme oxygenase-1 activity in vitro. We demonstrate that inhibition of HO1 reflects an interaction of MGd with NADPH-cytochrome P450 reductase, the electron donor for HO1, that results in diversion of reducing equivalents from heme oxidation to oxygen reduction. In accord with this mechanism, MGd is also an in vitro inhibitor of CYP2C9, CYP3A4, and CYP4A1. Inhibition of HO1 by MGd may contribute to its anticancer activity, whereas its in vitro inhibition of a broad spectrum of P450 enzymes indicates that a potential exists for drug-drug interactions.

Motexafin gadolinium (MGd; Xcytrin; Pharmacyclics, Inc., Sunnyvale, CA) is a pentaaza-coordinated expanded porphyrin with biological activity as an anticancer agent (Fig. 1A). It selectively localizes to cancerous cells (Young et al., 1996), a characteristic inherent to many porphyrins, and it facilitates their destruction through redox processes that generate reactive oxygen species (ROS) and deplete the cell of reducing factors (Magda et al., 2001, 2002). In the presence of ascorbate, NADPH, or glutathione, MGd is easily reduced [$E_{1/2}$(red) $\approx$ 0.08 V versus normal hydrogen electrode] (Ali and van Lier, 1999). Under aerobic conditions, MGd in turn reduces $O_2$ to superoxide, which can disproportionate to hydrogen peroxide (Fig. 1B). This redox cycling is only part of the toxicity of MGd, because enzymes with redox-active cysteine residues such as ribonucleotide reductase and thioredoxin reductase are inhibited by MGd with $IC_{50}$ values in the low micromolar range (Hashemy et al., 2006).

This work was supported by National Institute of Health Grants DK30297 and GM25515.

Article, publication date, and citation information can be found at http://molpharm.aspetjournals.org.

doi:10.1124/mol.106.028407.

Heme degradation is catalyzed by the microsomal enzyme HO1 and requires NADPH and $O_2$ for oxidative cleavage of the porphyrin ring at the $\alpha$-methylene carbon to produce $\alpha$-biliverdin, CO, and free iron (Ortiz de Montellano, 1998). NADPH-cytochrome P450 reductase (CPR) is required to mediate the flow of electrons from NADPH to HO1. The biliverdin product is subsequently reduced by biliverdin reductase (BVR) to bilirubin, a potent antioxidant (Stocker et al., 1987). HO1 is induced by a number of factors typical of cancer cells, including heme, oxidative stress, and hypoxia (Choi and Alam, 1996). The primary determinants of the substrate specificity of HO1 are the two propionate groups at C6 and C7 of the heme (Tomaro et al., 1984), although recently compounds based on azalanstat, a structure dissimilar to heme, have been shown to be effective HO1 inhibitors (Vlahakis et al., 2005).

Inhibition of HO1 has been shown to result in antitumor activity, presumably through inactivation of the antiapoptotic properties of the products of HO1 (Sahoo et al., 2002; Tanaka et al., 2003; Berberat et al., 2005). Because MGd is an expanded porphyrin with some structural resemblance to

**ABBREVIATIONS:** MGd, motexafin gadolinium; ROS, reactive oxygen species; HO1, heme oxygenase-1; CPR, NADPH-cytochrome P450 reductase; BVR, biliverdin reductase; HPLC, high-performance liquid chromatography; SnPPIX, tin protoporphyrin IX; CI, combination index; SOD, superoxide dismutase.

heme and it is cytotoxic to some cell lines, we determined whether MGd is capable of inhibiting HO1 (Chen et al., 2005). We have found that MGd is only cytotoxic to hematopoietic cell lines that express HO1 constitutively. We have also determined the inhibitory effects of MGd on HO1 under a variety of in vitro conditions. We conclude that the high electron affinity of the molecule rather than its structural similarities to heme lead to inhibition of HO1 activity. This inhibition is starkly greater in the presence of CPR. Because CPR is the mandatory electron donor for almost all human cytochrome P450 enzymes, we have also examined the effects of MGd on the catalytic turnover of these enzymes. We have found that MGd is also an active inhibitor of cytochrome P450 enzymes, although with a lower potency than that exhibited for inhibition of HO1. This suggests that MGd may inhibit a broad range of enzymes that depend on $O_2$ and cellular reducing equivalents for activity. The interplay of HO1 and MGd may therefore be highly relevant to the anticancer action of MGd.

## Materials and Methods

**Materials.** Sodium ascorbate, deferoxamine, hemin, NADPH, and glucose 6-phosphate were purchased from Sigma-Aldrich (St. Louis, MO). Methanol (HPLC grade) was from Fisher Scientific Co. (Pittsburgh, PA). MGd was formulated by Pharmacyclics, Inc. as a 2 mM stock solution in 5% aqueous mannitol. SnPPIX dichloride was from Frontier Scientific, Inc. (Logan, UT).

**Cell Line and Growth Conditions.** HF-1, Ramos, DHL-4, DB, and Raji are B-cell-derived tumor lines. HL-60 is a myeloid line, whereas Jurkat and HuT78 are T-cell-derived. Wil-2 is a B-lymphoblastoid cell line. All cell lines were grown in RPMI 1640 medium with 10% fetal bovine serum in a 5% $CO_2$/air incubator at 37°C. For assays determining HO1 induction, growth inhibition, or apoptosis, cells were treated with 50 $\mu$M MGd for 24 h before analysis.

**Analysis of MGd-Treated Cells.** Cell numbers were determined using a model Z2 counter (Beckman Coulter, Miami, FL). Annexin V binding and propidium iodide exclusion were assayed with a FACSCalibur instrument (BD Biosciences, San Jose, CA) using reagents from BioVision (Mountain View, CA) per the manufacturer's protocol.

For drug combination studies, cytotoxicity was evaluated using annexin V staining. These data were then entered into CalcuSyn software (Biosoft, Ferguson, MO) for analysis by the combination index (CI) method of Chou and Talalay (1983) to determine synergism (CI $<$ 1), additivity (CI = 1), or antagonism (CI $>$ 1).

**Western Blotting for Heme Oxygenases.** Cells were lysed in triple-detergent lysis buffer (50 mM Tris-Cl, pH 8.0, 150 mM NaCl, 0.1% SDS, 0.5% deoxycholic acid, and 1.0% Nonidet P-40, supplemented with 1 mM phenylmethylsulfonyl fluoride and the Complete protease inhibitor cocktail (Roche Molecular Biochemicals, Indianapolis, IN) on ice for 10 min. After centrifugation at 10,000*g* for 10 min, the protein concentration was quantitated in the supernatant, and equal quantities of protein were resolved on the appropriate percentage SDS-polyacrylamide gels (Bio-Rad, Hercules, CA). Gels were transferred to polyvinylidene difluoride membranes using a semidry transfer cell (Bio-Rad) and Western blotting was performed using primary and anti-mouse and anti-rabbit secondary antibodies conjugated to Alexa Fluor 680 (Invitrogen, Carlsbad, CA) and IRdye800 (Rockland, Gilbertsville, PA), respectively. All membranes were blotted with an anti-Hsc70 (Santa Cruz Biotechnology, Inc., Santa Cruz, CA) antibody to control for loading and transfer. Bands were imaged and quantified in the linear range and normalized to Hsc70, using an Odyssey infrared imaging system (LI-COR, Lincoln, NE).

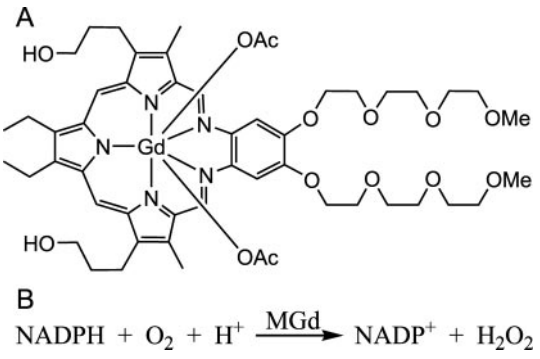


**Fig. 1.** A, structure of MGd. B, reaction catalyzed by MGd with $O_2$ and reducing equivalents from NADPH.

**Enzymes.** Truncated human HO1 lacking the 23 C-terminal residues was expressed, purified, and reconstituted with heme as described previously (Wilks et al., 1995). Human CPR was expressed and purified according to published procedures (Dierks et al., 1998), and CYP4A1 was expressed and purified as described previously (Hoch et al., 2000). Vivid CYP3A4 and CYP2C9 screening kits were purchased from Invitrogen. Catalase, SOD, glucose-6-phosphate dehydrogenase, cytochrome *c*, and protocatechuate 3,4-dioxygenase were purchased from Sigma-Aldrich.

**Spectroscopic Methods.** Spectroscopic assays were performed on an 8453 diode array spectrophotometer (Agilent Technologies, Palo Alto, CA) in 0.1 M potassium phosphate buffer, pH 7.4, at room temperature (~22°C). The final concentrations in the assays were 1 $\mu$M human CPR, 200 $\mu$M NADPH, and 10 $\mu$M MGd. The NADPH regenerating system consisted of 5 mM glucose 6-phosphate and 1 unit/ml glucose-6-phosphate dehydrogenase. The rates of NADPH and MGd consumption were measured by monitoring the absorption decrease at 340 nm ($\varepsilon$ = 6.22 $mM^{-1}$ $cm^{-1}$) and 470 nm ($\varepsilon$ = 85 $mM^{-1}$ $cm^{-1}$) for NADPH and MGd, respectively. To measure the stoichiometry of NADPH consumption by MGd, assays containing 400 $\mu$M NADPH and 1 $\mu$M CPR were mixed with repeated additions of 2 $\mu$M MGd. The amounts of NADPH and MGd consumed for each addition were compared.

**Measurement of HO1 Activity by HPLC.** Assays were carried out in 300 $\mu$l of a solution containing 0.1 M potassium phosphate buffer, pH 7.4, 1 $\mu$M HO1, 10 $\mu$M heme, and either 1 $\mu$M CPR, 1 mM NADPH, 5 mM glucose 6-phosphate, and 1 unit/ml glucose-6-phosphate dehydrogenase or 10 mM sodium ascorbate plus 2 mM deferoxamine. The inhibitor (MGd or SnPPIX) concentrations ranged from 0.1 to 100 $\mu$M. In one set of experiments, 10 $\mu$g/ml catalase and 17 units/ml SOD were included. Each reaction was preincubated in the dark for 10 min at room temperature followed by 15-min incubation after addition of the reductant. The reaction was quenched with two drops of 37% hydrochloric acid and three drops of acetic acid and was extracted with 700 $\mu$l of $CH_2Cl_2$. The organic phase was washed with 700 $\mu$l of water and evaporated under a stream of air. The resulting residue was dissolved in 500 $\mu$l of methanol [5% $H_2SO_4$ (v/v)] and was maintained at 4°C for at least 8 h in the dark. The dimethyl-esterified biliverdin was extracted with 700 $\mu$l of $CHCl_3$. The organic phase was washed with water (2 $\times$ 700 $\mu$l) and was then evaporated to dryness under a stream of air. The residue was dissolved in 70% methanol and was loaded onto a YMC ODS-AQ column (S-5, 120 Å, 4.5 $\times$ 250 mm). Solvents A and B were water and methanol, respectively. The HPLC running conditions were as follows: flow rate, 1.0 ml/min; 30% B for 5 min, 30 to 70% B in 0.1 min, 70 to 95% B in 25 min, 95% B for 7 min, 95 to 30% B in 1 min, and finally 30% B for 20 min. The eluent was monitored at 375 nm and was referenced against the absorption at 598 nm.

**Cytochrome *c* Reduction Assay.** Reactions contained 0.1 M potassium phosphate buffer, pH 7.4, 1 $\mu$M HO1, 10 $\mu$M heme, 1 mM NADPH, and 10 $\mu$M MGd in the presence and absence of 1 $\mu$M CPR. After 15 min, an aliquot of the reaction was diluted 100-fold into a 100-$\mu$l assay mixture within a cuvette containing 40 $\mu$M cytochrome *c* and 200 $\mu$M NADPH, so that the final concentration of CPR was 10

nM and of MGd was 100 nM. The increase in absorbance at 550 nm was monitored over 2 min, and the rate of cytochrome *c* reduction was calculated using an extinction coefficient for reduced cytochrome *c* of 21 $mM^{-1}$ $cm^{-1}$ (Margoliash and Walasek, 1967).

**$O_2$ Electrode Measurements.** An Oxy5 oxygraph electrode (Gilson, Inc., Middleton, WI) was used at 22°C. The assays contained 0.1 M potassium phosphate buffer, pH 7.4, 1 $\mu$M HO1, 10 $\mu$M heme, and either 1 $\mu$M CPR, 1 mM NADPH, 5 mM glucose 6-phosphate, 1 unit/ml glucose-6-phosphate dehydrogenase, and 10 $\mu$M MGd or 10 mM sodium ascorbate, 2 mM deferoxamine, and 400 $\mu$M MGd. A dissolved $O_2$ concentration of 270 $\mu$M was used based on calibration of the electrode by consuming a known concentration of protocatechuate with protocatechuate 3,4-dioxygenase (Wittaker et al., 1990). Assays to measure the stoichiometry of $O_2$ consumption by MGd containing 1 mM NADPH and 1 $\mu$M CPR were mixed with repeated additions of 2 $\mu$M MGd.

**Cytochrome P450 Activity Assays.** The activity of CYP4A1 was measured by lauric acid $\omega$-hydroxylation. The incubations were performed as described previously (Hoch et al., 2000), and the reaction mixtures were worked up by solid phase extraction and analyzed by gas chromatography-mass spectrometry (He et al., 2005). The activities of CYP3A4 and CYP2C9 were measured with Vivid CYP3A4 and CYP2C9 green screening kits (Invitrogen). These kits use direct fluorometric assays in a 96-well plate format and were carried out according to the manufacturer's instructions. Wells that did not contain an inhibitor but contained the complete enzyme system plus the fluorescent substrate were used as "100% activity" controls (i.e., uninhibited enzyme activity). The other wells were identical except for the presence of the inhibitor. When indicated in the text, catalase or an NADPH-regenerating system was included in the wells. At the completion of the reactions, the CYP3A4 and CYP2C9 activities were read on a microplate fluorometer (Spectra Max, Sunnyvale, CA) with the excitation set at 485 nm and the emission at 530 nm. The data are expressed as a percentage of the maximum control fluorescence level.

**Data Analysis.** To determine the $IC_{50}$ values, the percentage of inhibition data were fitted to the equation below by nonlinear regression using the program KaleidaGraph (Abelbeck/Synergy Software, Reading, PA): $p = p_{max} + \{(p_{min} - p_{max})/[1 + (I/IC_{50})^{nH}]\}$, where $p$ (percentage of inhibition) is the relative decrease in enzyme activity due to the inhibitor concentration $I$, $n$ is the Hill coefficient, $p_{max} \leq 100$, and $p_{min} \geq 0$.

## Results

**Cell Lines Expressing HO1 Constitutively Are Sensitive to Induction of Apoptosis by MGd.** MGd is a so-called expanded porphyrin (in the texaphyrin family) that contains five nitrogens in the central core instead of the four found in heme (Fig. 1A). Its ability to redox cycle (Fig. 1B) may induce cell death in sensitive cell lines. Similar to other porphyrins, MGd could potentially induce expression and/or inhibit the activity of HO1. We treated eight hematopoietic tumor-derived cell lines with MGd to determine whether it resulted in increased expression of HO1 protein. In Wil-2 and Ramos cell lines, HO1 expression increased 2- and 8-fold, respectively, whereas no increase was detected in the other six cell lines (Fig. 2A). It is noteworthy that the two cell lines (HF-1 and Wil-2) that expressed detectable levels of HO1 in the absence of MGd were sensitive to MGd-induced apoptosis, whereas the six cell lines that did not constitutively express HO1 did not show similar sensitivity (Fig. 2B). It is possible that one or more of the cell lines that show no expression of HO1, either in the absence or presence of MGd, do not have the ability to express HO1. Furthermore, the reason for their lack of sensitivity to MGd is unclear, because CPR was present at similar levels in all the cell lines (data not shown), but it presumably involves the action of alternative protective mechanisms.

**MGd Synergizes with SnPPIX to Kill Cells.** One possible explanation for the correlation between constitutive

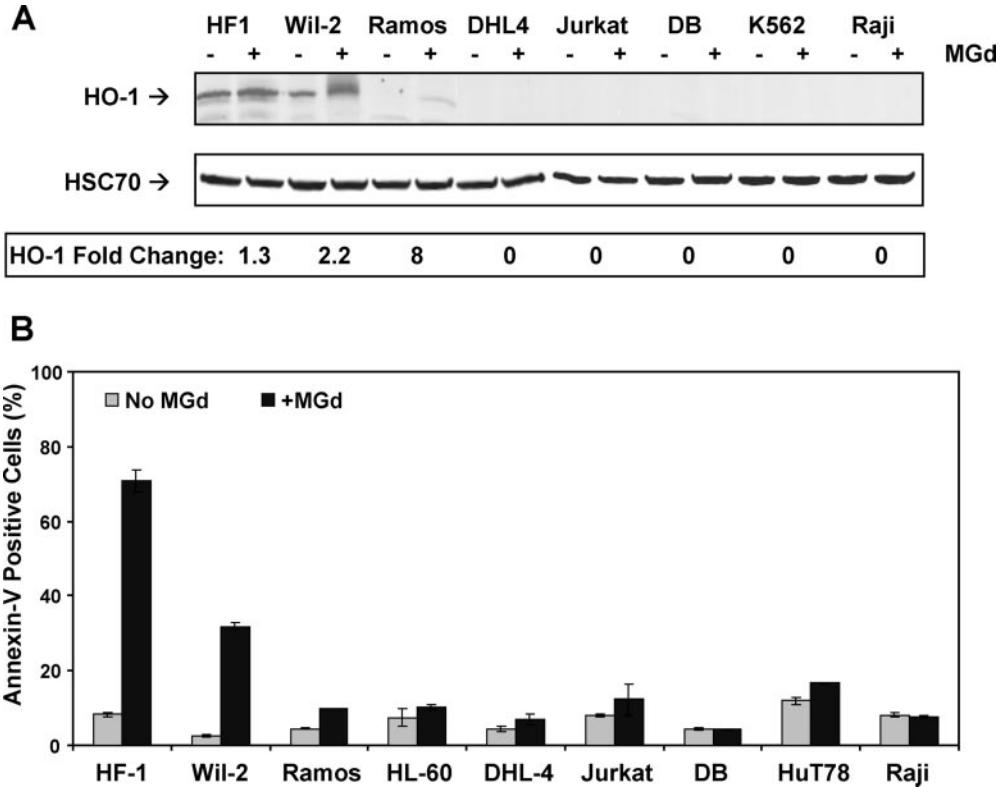


**Fig. 2.** A, Western blot for HO1 in MGd-treated hematopoietic tumor-derived cell lines. Cells were grown in the presence (+) or absence (−) of 50 $\mu$M MGd for 24 h. Protein extracts were separated by SDS-polyacrylamide gel electrophoresis, and Western blotting was performed with antibodies to HO1. Hsc70 was used as an internal loading standard. B, cells were grown in the presence (+) or absence (−) of 50 $\mu$M MGd for 4 days. Numbers of apoptotic cells were quantitated by fluorescein isothiocyanate-annexin V binding using flow cytometry.

expression of HO1 and sensitivity to MGd-induced apoptosis is that MGd might inhibit HO1 activity. Although unlikely based on structural features, another potential explanation is that HO1 degrades MGd into toxic metabolites. To distinguish between these two possibilities, we used SnPPIX to inhibit HO1 activity. If MGd is an inhibitor of HO1, then it might be expected to be more toxic in combination with SnPPIX. However, if HO1 activity is required to metabolize MGd into a toxic metabolite, then the combination of MGd and SnPPIX would be expected to be less toxic than MGd alone. Treatment of HF-1 cells with various combinations of MGd and SnPPIX showed substantially greater killing of cells than treatment with either agent alone as assessed by a marker of apoptosis, annexin V, after 24 h (Fig. 3A). The combination index of <1 revealed that treatment with MGd and SnPPIX resulted in synergistic killing (Fig. 3B). Combinations of MGd and SnPP that individually induced minimal apoptosis above background were also synergistic in inducing apoptosis after 4 days (data not shown). These data are consistent with the possibility that MGd inhibits HO1 activity, thereby resulting in cell death

**CPR Catalyzed MGd Metabolism.** MGd shows significant absorbance at 470 and 740 nm, wavelengths at which HO1 activity can be monitored through the formation of biliverdin (688 nm) or in the BVR-coupled assay through the formation of bilirubin (468 nm). In the presence of MGd, no detectable bilirubin formation was observed at 468 nm in the HO1-BVR-coupled assay; instead, there was a rapid decay of the 340-nm NADPH peak and the 470- and 740-nm peaks of MGd (data not shown). Removing HO1, heme, and BVR from the assays had no effect on the rate of NADPH and MGd disappearance. In our assays, reaction of 200 $\mu$M NADPH with 10 $\mu$M MGd in potassium phosphate buffer, pH 7.4, shows a linear rate of 5 $\mu$M $min^{-1}$ that increases dramatically to 300 $\mu$M $min^{-1}$ upon addition of 1 $\mu$M CPR. This is faster than the initial rate of 0.7 $\mu$M $min^{-1}$ previously reported with 250 $\mu$M NADPH and 12.5 $\mu$M MGd in HEPES/NaCl, pH 7.5, buffer (Magda et al., 2001). Electron transfer from NADPH to MGd is accelerated by the presence of CPR to such a degree that all of the available NADPH is consumed in an apparent first-order reaction with a half-life of 15 s, whereas some MGd remains (Fig. 4A). To prevent rapid depletion of NADPH, a glucose-6-phosphate dehydrogenase regenerating system was included in the assays. In this situation, the concentration of NADPH remains fixed, whereas all of the MGd is consumed within 1 min (Fig. 4B). In the absence of NADPH, there was no CPR-dependent degradation of MGd.

**HO1 Inhibition.** We used quenched HPLC assays to detect biliverdin formation by HO1 in the presence of either MGd or the strong competitive inhibitor SnPPIX (Fig. 5) (Drummond and Kappas, 1982). Under the conditions of our assays, MGd was a more effective inhibitor, exhibiting 90% inhibition at 10 $\mu$M MGd compared with SnPPIX, which gave 50% inhibition at the same concentration (Fig. 6). To determine whether CPR was necessary for MGd inhibition of HO1, we used sodium ascorbate as the alternate electron donor in

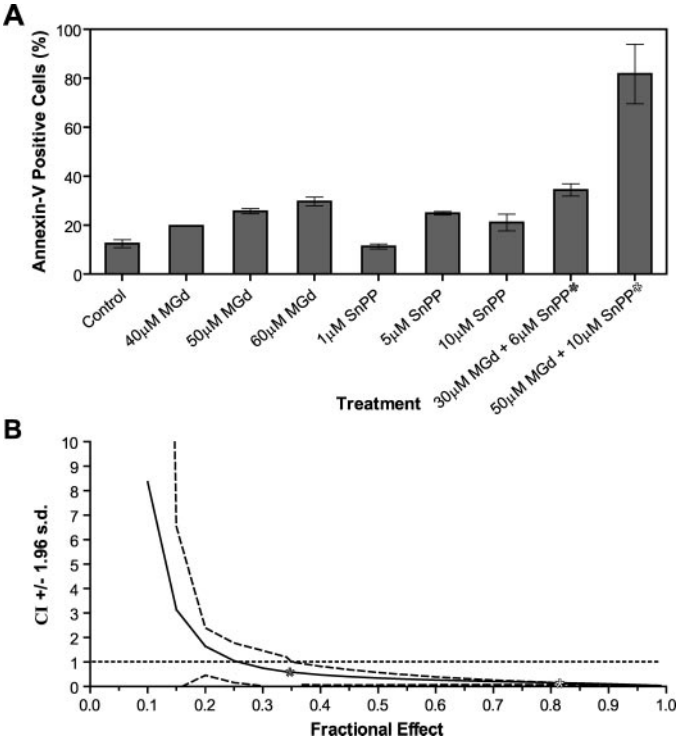


**Fig. 3.** A, MGd and SnPPIX synergize to kill HF-1 cells. HF-1 cells were treated with various concentrations of MGd, SnPPIX, or combinations of the drugs for 24 h. Apoptosis was quantitated by assay for annexin V binding. B, CI plot showing CI < 1, consistent with synergistic interaction between MGd and SnPPIX. The center curve is the calculated CI with the boundary lines representing ± 1.96 SDs for 95% certainty.

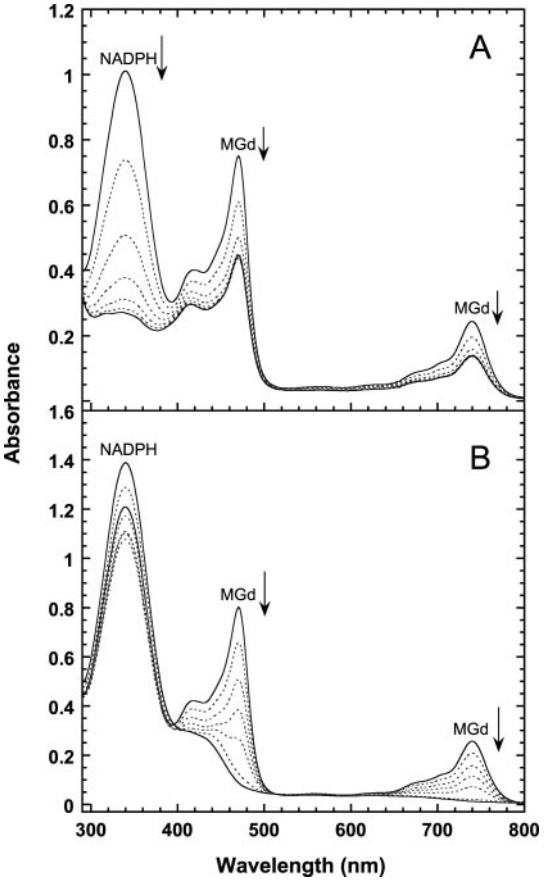


**Fig. 4.** A, Spectroscopic changes in the presence of 200 $\mu$M NADPH, 1 $\mu$M CPR, and 10 $\mu$M MGd, showing an initial rate of NADPH consumption of 300 $\mu$M/min and MGd consumption of 11 $\mu$M/min. B, addition of the NADPH regeneration system maintains NADPH levels, whereas MGd consumption shows the same initial rate of disappearance. The time scale of the reactions was 60 s, with spectra shown at 10-s intervals.

the HO1-coupled oxidation reaction. Here, SnPPIX maintains the same level of inhibition, whereas MGd is much less effective, suggesting an alternate mechanism of inhibition from SnPPIX that is amplified in the presence of CPR. Aqueous mannitol (5%) serves as a stabilizer in the solvent in which the MGd was provided, and it had no effect on HO1 activity in the absence of MGd (data not shown). MGd inhibits its HO1 activity with $IC_{50}$ = 0.2 $\mu$M (Fig. 7). Catalase has been found to prevent MGd cell toxicity in vivo (Evens et al., 2005a). Addition of catalase plus SOD to the assays to prevent deleterious ROS from degrading heme and interfering with the reaction (Nagababu and Rifkind, 2004) gives rise to only a small recovery of activity with a corresponding increase in the $IC_{50}$ to 0.3 $\mu$M. In contrast, MGd is a much less potent inhibitor ($IC_{50}$ = 4.6 mM) in the reaction supported by ascorbate than in that supported by NADPH/CPR.

CPR activity, as measured by the reduction of cytochrome *c* after the full time course of the HO1 activity assays (15 min), was unaffected by concentrations of MGd at which significant HO1 inhibition was observed. Therefore, inactivation of the electron transfer properties of CPR is ruled out, and HO1 is likely to be inhibited by either a limiting $O_2$ concentration or by metabolites produced in the CPR-dependent degradation of MGd, which was previously shown to produce free $Gd^{3+}$ and the nonaromatic four-electron reduced macrocycle (Mani et al., 2005).

**$O_2$ Consumption.** Using a Clark oxygen electrode, we measured the change in the dissolved $O_2$ concentration under conditions that result in 90% inhibition of HO1. Upon addition of 10 $\mu$M MGd, the concentration of dissolved $O_2$ decreased rapidly and was completely consumed within 1 min (Fig. 8). Over the remaining time course of the assay (15 min), the concentration of dissolved $O_2$ returned to >50% of the original concentration through diffusion of new $O_2$ into the reaction chamber. Using ascorbate as the electron donor, 400 $\mu$M MGd results in 40% inhibition of HO1 and was sufficient to decrease the concentration of dissolved $O_2$ to approximately 40% of the starting concentration.

In the presence of CPR the stoichiometry of NADPH and $O_2$ consumption is severely uncoupled from MGd consumption. The amount of NADPH and $O_2$ consumed was correlated with the amount of MGd to determine the stoichiometry of the reaction. Approximately 38 ± 2 equivalents of NADPH and 42 ± 5 equivalents of $O_2$ were consumed for every MGd that was lost.

**Cytochrome P450 Inhibition.** CPR is required for the catalytic activities of other enzymes, most notably for turnover of the cytochrome P450 enzymes. We have therefore

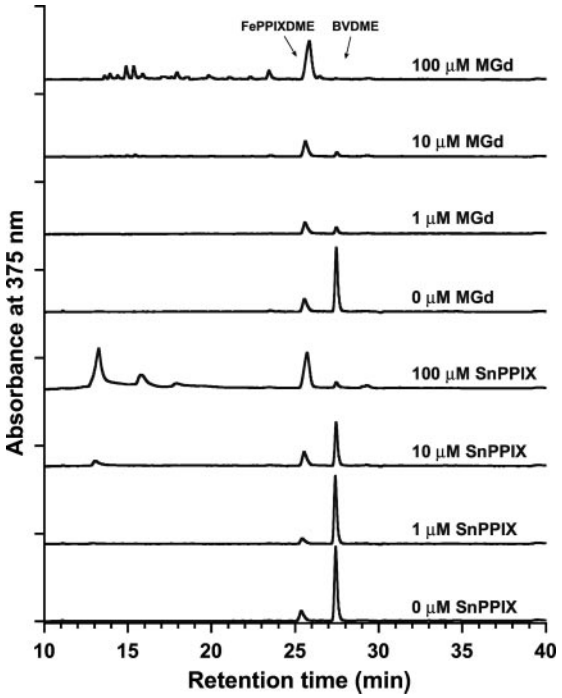


**Fig. 5.** HPLC chromatogram showing MGd and SnPPIX inhibition of HO1. Assays contained 1 $\mu$M HO1, 10 $\mu$M heme, 1 $\mu$M CPR, 1 mM NADPH, 5 mM glucose 6-phosphate, 1 unit/ml glucose-6-phosphate dehydrogenase and the indicated amount of inhibitor. Unreacted heme elutes as the FePPIX dimethyl ester (FePPIXDME) at ~26 min and biliverdin dimethyl ester (BVDME) at ~28 min.

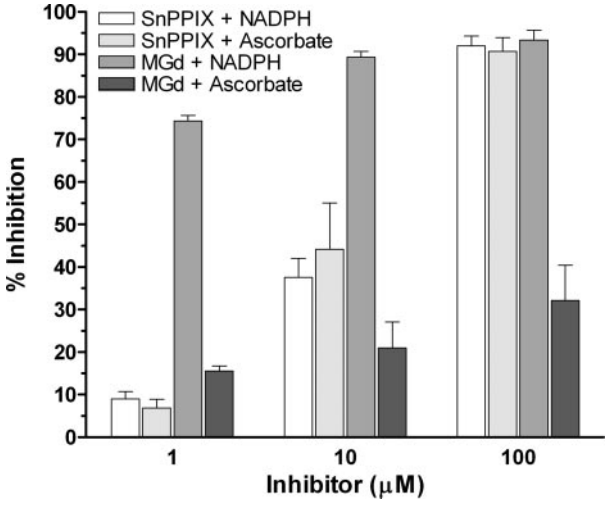


**Fig. 6.** Relative inhibition of HO1 in the presence of SnPPIX or MGd with either NADPH/CPR or ascorbate as the electron donor.

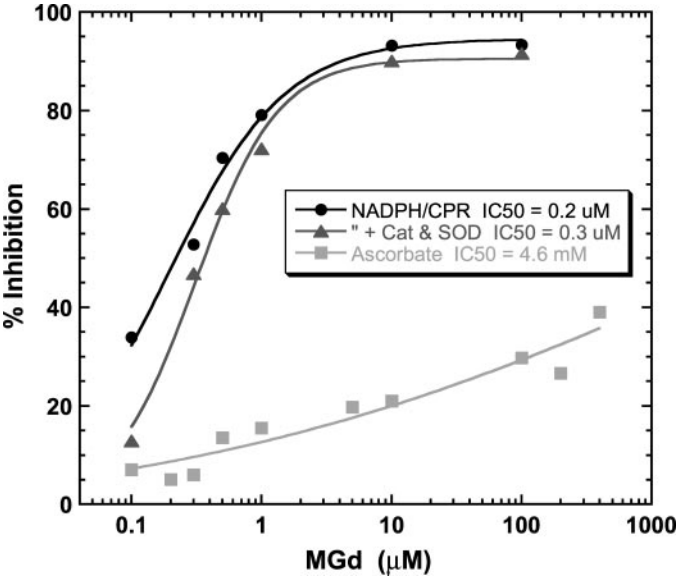


**Fig. 7.** MGd inhibition of HO1 activity with NADPH/CPR in the presence (▲) and absence (●) of 10 $\mu$g/ml catalase and 17 units/ml SOD gives $IC_{50}$ values of 0.3 and 0.2 $\mu$M, respectively. Assays contained 1 $\mu$M HO1, 10 $\mu$M heme, and either 1 $\mu$M CPR, 1 mM NADPH, and an NADPH regenerating system or 10 mM sodium ascorbate and 2 mM deferoxamine. Using ascorbate as the reductant (■) the $IC_{50}$ increases to 4.6 mM.

investigated whether MGd, through its action on CPR, inhibits the catalytic activities of cytochrome P450 enzymes. Three P450 enzymes, CYP2C9, CYP3A4, and CYP4A1, were selected for these inhibition studies. CYP2C9, and particularly CYP3A4, are responsible for a large proportion of all drug oxidations mediated by the human P450 system (Guengerich, 2005), whereas CYP4A1 is a representative of the class of P450 enzymes responsible for the formation of 20-HETE, an arachidonic acid-derived endogenous vasocontrictor (Capdevila et al., 2005). The inhibition of CYP4A1-mediated lauric acid $\omega$-hydroxylation by MGd was measured in 100 $\mu$M potassium phosphate buffer, alone or in the presence of 10 $\mu$g/ml catalase or an NADPH regenerating system. At MGd concentrations of 10 and 100 $\mu$M, 34 and 98% inhibition was observed, respectively, with similar inhibitory potencies in the three different incubation systems. The $IC_{50}$ values for CYP4A1, CYP3A4, and CYP2C9 measured in the presence of the NADPH regenerating system were 16, 7, and 3 $\mu$M, respectively, all of which are substantially higher values than for the inhibition of HO1 (Fig. 9).

## Discussion

MGd, which shows promise as a single agent or in combination with radiotherapy, is now in phase II and III clinical trials (Meyers et al., 2004; Evens et al., 2005b). Some of its anticancer action seems to be due to the formation of ROS that induce necrosis or apoptosis (Evens et al., 2005a). However, many cancer cells are hypoxic and/or contain high concentrations of HO1, a protective enzyme that has been linked to rapid tumor growth as a result of its antioxidative and antiapoptotic properties (Tanaka et al., 2003). HO1 is induced under a number of conditions that cause stress to the cell, including hypoxia, heavy metals, UV radiation, and ROS (Choi and Alam, 1996). The protection conferred by induction of HO1 results not only from a decrease in the deleterious effects of free heme, which include lipid peroxidation and oxygen free radical formation but also from the properties of bilirubin and CO, the end products of heme metabolism. Bilirubin is a potent free radical scavenger (Stocker et al., 1987), whereas CO is a signaling molecule that activates pathways that reduce hypertension and increase blood flow to tissues (Kim et al., 2006). There is evidence that HO1 inhibition is cytotoxic and can increase sensitivity of tumor cells to anticancer treatments (Sahoo et al., 2002; Tanaka et al., 2003; Berberat et al., 2005).

Here, we show a correlation between HO1 expression and sensitivity to MGd-induced apoptosis, suggesting that MGd might inhibit HO1 activity and thus promote cell death. We provide in vitro evidence that MGd inhibits HO1 and demonstrate that this inhibition results from interaction of MGd with the microsomal electron transfer protein CPR. This interaction, which diverts electrons into the reduction of $O_2$, results in the depletion of NADPH and $O_2$ and production of ROS (Fig. 1B). MGd did not interact directly with HO1, and it was not metabolized by this enzyme. Although HO1 has some tolerance for substrate alterations (Ortiz de Montellano and Wilks, 2001), MGd is either too large to fit into the catalytic site or it does not satisfy specific requirements for binding within that site. In HO1, the heme is sandwiched between two $\alpha$-helices and electrostatic interactions between the heme propionates and basic residues at the protein surface confer substrate specificity and reactivity (Schuller et al., 1999). Although zinc protoporphyrin IX pegylated at the positions normally occupied by the propionate groups can inhibit HO1 with a potency similar to that of ZnPPIX (Sahoo et al., 2002), the more extensively altered structure of MGd is apparently incompatible with competitive binding to the protein. Nonetheless, MGd is a strong inhibitor with an $IC_{50}$ in the low micromolar range.

In the presence of NADPH, CPR, and $O_2$, MGd is degraded at an accelerated rate by a process that consumes many equivalents of NADPH and $O_2$ for each MGd that is metabolized. This reaction depletes the necessary cofactor (NADPH) and one of the substrates ($O_2$) required for heme

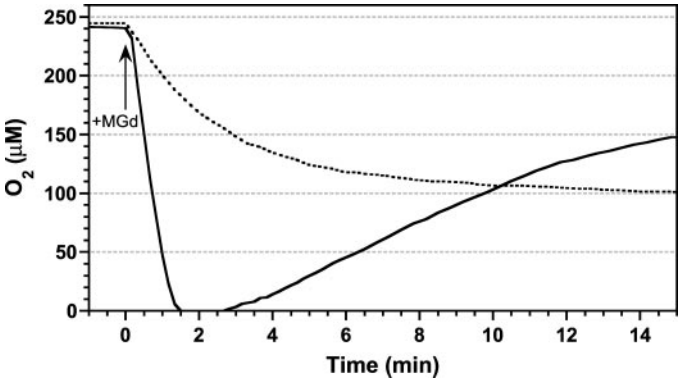


**Fig. 8.** Oxygen electrode trace showing the consumption of $O_2$ upon addition of 10 $\mu$M MGd to a reaction containing 1 $\mu$M HO1, 10 $\mu$M heme, 1 $\mu$M CPR, 1 mM NADPH, 5 mM glucose 6-phosphate, and 1 unit/ml glucose-6-phosphate dehydrogenase (solid line) or 400 $\mu$M MGd to a reaction containing 1 $\mu$M HO1, 10 $\mu$M heme, 10 mM ascorbate, and 2 mM DFA (dotted line). Omission of HO1 and heme from the assays resulted in similar $O_2$ consumption profiles (data not shown).

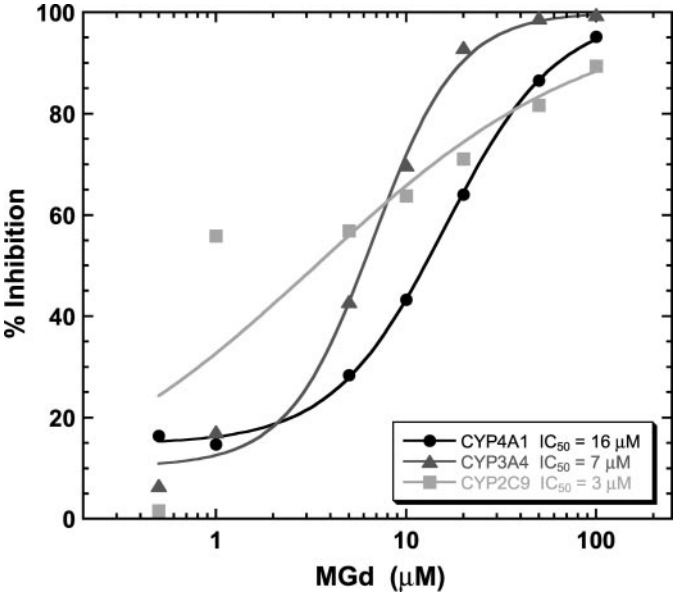


**Fig. 9.** MGd inhibition of CYP4A1 (●), CYP3A4(▲), and CYP2C9 (■) activity in a system consisting of NADPH/CPR plus the NADPH regenerating system. The $IC_{50}$ values of MGd in these three systems are 16, 7, and 3 $\mu$M, respectively. CYP4A1 assays contained 100 $\mu$M lauric acid, 0.1 $\mu$M CYP450, 1 mM NADPH, 1 $\mu$M CPR, and the NADPH regenerating system. CYP3A4 and CYP2C9 assays contained 5 and 10 nM CYP450 BACULOSOMES reagent (PanVera Corp., Madison, WI), respectively, 2 $\mu$M Vivid CYP450 substrate (PanVera Corp.), 100 $\mu$M $NADP^+$, and regeneration system.

oxygenase activity. Previous work has shown that CPR-catalyzed degradation of MGd produces free $Gd^{3+}$ and the four-electron reduced expanded porphyrin (Mani et al., 2005). We have found the stoichiometry of this process to be ~40:40:1 (NADPH/$O_2$/MGd), a ratio that requires a large number of electrons to flow from NADPH into $O_2$ in an uncoupled manner. MGd thus prefers to react with NADPH indirectly, presumably by accepting one electron at a time from CPR after the NADPH electrons are uncoupled by the flavin prosthetic groups of this enzyme.

CPR is the electron transfer system in the endoplastic reticulum that supplies the reducing equivalents required by both the heme oxygenases and P450 enzymes (Murataliev et al., 2004). The distribution of CPR in human tissues is thus correlated with that of both the HO and P450 enzymes. CPR contains two tightly bound flavin cofactors, an FAD and an FMN (Wang et al., 1997). The FAD accepts two electrons from NADPH, whereas the FMN serves as a one-electron carrier. The ease with which CPR performs one-electron transfers makes it responsible for the toxicity of other reducible compounds, including the antitumor drug doxorubicin and the herbicide paraquat (Smith, 1987; Bartoszek, 2002). In each case, CPR activates them to toxic metabolites via a one-electron reduction. Furthermore, under aerobic conditions, reduced paraquat reacts with $O_2$ to generate superoxide in a cycle that depletes the intracellular NADPH (Lock and Wilks, 2001).

Other molecules that both inhibit and induce HO1 include NO and SnPPIX. Both molecules induce HO1 through the propagation of free radical cascades. NO inhibits HO1 by binding to the heme iron in place of $O_2$ (Wang et al., 2003), whereas SnPPIX competes with heme for binding to the active site (Valaes et al., 1998). The latter has been used to treat neonatal hyperbilirubinemia.

The cytochromes P450 are heme-thiolate-containing monooxygenases that are involved in the biosynthesis of various endogenous factors as well as in the metabolism of most drugs and xenobiotics (Guengerich, 2005). The cytochrome P450 enzymes, except for some steroidogenic isoforms, use two electrons provided by CPR for the activation of $O_2$ in their catalytic cycle. CYP3A4 and CYP2C9 are the major P450 enzymes in human liver and intestine (Guengerich, 2005), whereas CYP4A1 catalyzes the $\omega$-hydroxylation of lauric acid and other fatty acids, including arachidonic acid (Capdevila et al., 2005). P450 enzymes do not seem to play a role in the metabolism of MGd (Mani et al., 2005). Nevertheless, MGd is a highly effective inhibitor of CYP2C9, CYP3A4, and CYP4A1, the three forms examined here. Because inhibition of these enzymes also involves diversion of electrons from CPR into uncoupled $O_2$ reduction, with a consequent depletion of NADPH and oxygen, it is very likely that MGd will also inhibit other CPR-dependent P450 enzymes, at least in vitro. Differential inhibition of the three enzymes may reflect a difference in their oxygen affinities or their ability to undergo superoxide-dependent turnover. If MGd were to inhibit P450 enzymes in vivo, it might alter the metabolism of other drugs. The physiological relevance of the potential P450 inhibition by MGd is not clear, because in more than 500 patients who have received MGd in various clinical trials, no concerns have been raised about potential drug-drug interactions.

MGd disrupts a number of key enzymes important in cellular processes, leading to an increase in intracellular free zinc and metallothionein production (Lecane et al., 2005; Magda et al., 2005). It also inhibits thioredoxin reductase, an important antioxidant defense, and ribonucleotide reductase, an enzyme important in DNA synthesis (Hashemy et al., 2006). The ability of MGd to increase oxidative stress to tumor cells and simultaneously inhibit HO1 and other critical enzymes may contribute to its effectiveness as an anticancer agent.



## References


Ali H and van Lier JE (1999) Metal complexes as photo- and radiosensitizers. *Chem Rev* **99:**2379–2450.

Bartoszek A (2002) Metabolic activation of adriamycin by NADPH-cytochrome P450 reductase: overview of its biological and biochemical effects. *Acta Biochim Pol* **49:**323–331.

Berberat PO, Dambrauskas Z, Gulbinas A, Giese T, Giese N, Künzli B, Autschbach F, Meuer S, Büchler MW, and Friess H (2005) Inhibition of heme oxygenase-1 increases responsiveness of pancreatic cancer cells to anticancer treatment. *Clin Cancer Res* **11:**3790–3798.

Capdevila JH, Holla VR, and Falck JR (2005) Cytochrome P450 and the metabolism and bioactivation of arachidonic acid and eicosanoids, in *Cytochrome P450: Structure, Mechanism, and Biochemistry*, 3rd ed. (Ortiz de Montellano PR ed) pp 531–551, Plenum, New York.

Chen C, Ramos J, Sirisawad M, Miller R, and Naumovski L (2005) Motexafin gadolinium-induces mitochondrially-mediated caspase-dependent apoptosis. *Apoptosis* **10:**1131–1142.

Choi AM and Alam J (1996) Heme oxygenase-1: function, regulation, and implication of a novel stress-inducible protein in oxidant-induced lung injury. *Am J Respir Cell Mol Biol* **15:**9–19.

Chou T-C and Talalay P (1983) Analysis of combined drug effects: a new look at a very old problem. *Trends Pharmacol Sci* **4:**450–454.

Dierks EA, Davis SC, and Ortiz de Montellano PR (1998) Glu-320 and Asp-323 are determinants of the CYP4A1 hydroxylation regiospecificity and resistance to inactivation by 1-aminobenzotriazole. *Biochemistry* **37:**1839–1847.

Drummond GS and Kappas A (1982) Chemoprevention of neonatal jaundice: potency of tin-protoporphyrin in an animal model. *Science (Wash DC)* **217:**1250–1252.

Evens AM, Lecane P, Magda. D, Prachand S, Singhal S, Nelson J, Miller RA, Gartenhaus RB, and Gordon LI (2005a) Motexafin gadolinium generates reactive oxygen species and induces apoptosis in sensitive and highly resistant multiple myeloma cells. *Blood* **105:**1265–1273.

Evens AM, Balasubramanian L, and Gordon LI (2005b) Motexafin gadolinium induces oxidative stress and apoptosis in hematologic malignancies. *Curr Treat Options Oncol* **6:**289–296.

Guengerich FP (2005) Human cytochrome P450 enzymes, in *Cytochrome P450: Structure, Mechanism, and Biochemistry*, 3rd ed. (Ortiz de Montellano PR ed) pp 377–530, Plenum, New York.

Hashemy SI, Ungerstedt JS, Avval FZ, and Holmgren A (2006) Motexafin gadolinium: a tumor selective drug targeting thioredoxin reductase and ribonucleotide reductase. *J Biol Chem* **281:**10691–10697.

He X, Cryle MJ, De Voss JJ, and Ortiz de Montellano PR (2005) Calibration of the channel that determines the $\omega$-hydroxylation regiopecificity of cytochrome P4504A1. Catalytic oxidation of 12-halododecanoic acids. *J Biol Chem* **280:**22697–22705.

Hoch U, Zhang Z, Kroetz DL, and Ortiz de Montellano PR (2000) Structural determination of the substrate specificities and regioselectivities of the rat and human fatty acid $\omega$-hydroxylases. *Arch Biochem Biophys* **373:**63–71.

Kim HP, Ryter SW, and Choi AM (2006) CO as a cellular signaling molecule. *Annu Rev Pharmacol Toxicol* **46:**411–449.

Lecane PS, Karaman MW, Sirisawad M, Naumovski L, Miller RA, Hacia JG, and Magda D (2005) Motexafin gadolinium and zinc induce oxidative stress responses and apoptosis in B-cell lymphoma lines. *Cancer Res* **65:**11676–11688.

Lock EA and Wilks MF (2001) Paraquat, in *Handbook of Pesticide Toxicology* (Krieger RI ed) pp 1559–1603, Academic Press, San Diego.

Magda D, Gerasimchuk N, Lecane P, Miller RA, Biaglow JE, and Sessler JL (2002) Motexafin gadolinium reacts with ascorbate to produce reactive oxygen species. *Chem Commun* 2730–2731.

Magda D, Lecane P, Miller RA, Lepp C, Miles D, Mesfin M, Biaglow JE, Ho VV, Chawannakul D, Nagpal S, et al. (2005) Motexafin gadolinium disrupts zinc metabolism in human cancer cell lines. *Cancer Res* **65:**3837–3845.

Magda D, Lepp C, Gerasimchuk N, Lee I, Sessler JL, Lin A, Biaglow JE, and Miller RA (2001) Redox cycling by motexafin gadolinium enhances cellular response to ionizing radiation by forming reactive oxygen species. *Int J Radiat Oncol Biol Phys* **51:**1025–1036.

Mani C, Upadhyay S, Lacy S, Boswell GW, and Miles DR (2005) Reductase-mediated metabolism of motexafin gadolinium (Xcytrin) in rat and human liver subcellular fractions and purified enzyme preparations. *J Pharm Sci* **94:**559–570.

Margoliash E and Walasek OF (1967) Cytochrome *c* from vertebrate and invertebrate sources. *Methods Enzymol* **10:**339–348.

Meyers CA, Smith JA, Bezjak A, Mehta MP, Liebmann J, Illidge T, Kunkler I, Caudrelier JM, Eisenberg PD, Meerwaldt J, et al. (2004) Neurocognitive function and progression in patients with brain metastases treated with whole-brain radiation and motexafin gadolinium: results of a randomized phase III trial. *J Clin Oncol* **22:**157–165.

Murataliev MB, Feyereisen R, and Walker A (2004) Electron transfer by diflavin reductases. *Biochim Biophys Acta***1698:**1–26.

Nagababu E and Rifkind JM (2004) Heme degradation by reactive oxygen species. *Antioxid Redox Signal* **6:**967–978.
Ortiz de Montellano PR (1998) Heme oxygenase mechanism: evidence for an electrophilic, ferric peroxide species. *Accounts of Chemical Research* **31:**543–549.
Ortiz de Montellano PR and Wilks A (2001) Heme oxygenase structure and mechanism, in *Iron Porphyrins*, *Advances in Inorganic Chemistry*: *Heme-Fe Proteins* (Sykes G and Mauk AG eds) pp 359–407, Academic Press, San Diego.
Sahoo SK, Sawa T, Fang J, Tanaka S, Miyamoto Y, Akaike T, and Maeda H (2002) Pegylated zinc protoporphyrin: a water-soluble heme oxygenase inhibitor with tumor-targeting capacity. *Bioconjug Chem* **13:**1031–1038.
Schuller DJ, Wilks A, Ortiz de Montellano PR, and Poulos TL (1999) Crystal structure of human heme oxygenase-1. *Nat Struct Biol* **6:**860–867.
Smith LL (1987) Mechanism of paraquat toxicity in lung and its relevance to treatment. *Hum Toxicol* **6:**31–36.
Stocker R, Yamamoto Y, McDonagh AF, Glazer AN, and Ames BN (1987) Bilirubin is an antioxidant of possible physiological importance. *Science (Wash DC)* **235:** 1043–1046.
Tanaka S, Akaike T, Fang J, Beppu T, Ogawa M, Tamura F, Miyamoto Y, and Maeda H (2003) Antiapoptotic affect of haem oxygenase-1 induced by nitric oxide in experimental solid tumor. *Br J Cancer* **88:**902–909.
Tomaro ML, Frydman RB, Frydman B, Pandey RK, and Smith KM (1984) The oxidation of hemins by microsomal heme oxygenase. Structural requirements for the retention of substrate activity. *Biochim Biophys Acta* **791:**342–349.
Valaes T, Drummond G, and Kappas A (1998) Control of hyperbilirubinemia in glucose-6-phosphate dehydrogenase-deficient newborns using an inhibitor of bilirubin production, Sn-mesoporphyrin. *Pediatrics* **101:**E1–E7.
Vlahakis JZ, Kinobe RT, Bowers RJ, Brien JF, Nakatsu K, and Szarek WA (2005) Synthesis and evaluation of azalanstat analogues as heme oxygenase inhibitors. *Bioorg Med Chem Lett* **15:**1457–1461.
Wang M, Roberts DL, Paschke R, Shea TM, Masters BSS, and Kim J-JP (1997) Three-dimensional structure of NADPH-cytochrome P450 reductase: prototype for FMN- and FAD-containing enzymes. *Proc Natl Acad Sci USA* **94:**8411–8416.
Wang J, Lu S, Moënne-Loccoz P, and Ortiz de Montellano PR (2003) Interaction of nitric oxide with human heme oxygenase-1. *J Biol Chem* **278:**2341–2347.
Wilks A, Black SM, Miller WL, and Ortiz de Montellano PR (1995) Expression and characterization of truncated human heme oxygenase (hHO-1) and a fusion protein of hHO-1 with human cytochrome P450 reductase. *Biochemistry* **34:**4421–4427.
Wittaker JW, Orville AM, and Lipscomb JD (1990) Protocatechuate 3,4-dioxygenase from *Brevibacterium fuscum*. *Methods Enzymol* **188:**82–88.
Young SW, Qing F, Harriman A, Sessler JL, Dow WC, Mody TD, Hemmi GW, Hao Y, and Miller RA (1996) Gadolinium(III) texaphyrin: a tumor selective radiation sensitizer that is detectable by MRI. *Proc Natl Acad Sci USA* **93:**6610–6615.

**Address correspondence to:** Dr. Paul Ortiz de Montellano, University of California, San Francisco, 600 16th St., San Francisco, CA 94143-2280. E-mail: ortiz@cgl.ucsf.edu